

Writer Identification and Writer Retrieval Based on NetVLAD with Re-ranking

ISSN 1751-8644
doi: 0000000000
www.ietdl.org

Shervin Rasoulzadeh¹, Bagher Babaali^{1*}

¹ School of Mathematics, Statistics and Computer Science, College of Science, University of Tehran, Tehran, Iran

* E-mail: babaali@ut.ac.ir

Abstract: This paper addresses writer identification and retrieval which is a challenging problem in the document analysis field. In this work, a novel pipeline is proposed for the problem by employing a unified neural network architecture consisting of the ResNet-20 as a feature extractor and an integrated NetVLAD layer, inspired by the vectors of locally aggregated descriptors (VLAD), in the head of the latter part. Having defined this architecture, triplet semi-hard loss function is used to directly learn an embedding for individual input image patches. Generalised max-pooling is used for the aggregation of embedded descriptors of each handwritten image. In the evaluation part, for identification and retrieval, re-ranking has been done based on query expansion and k -reciprocal nearest neighbours, and it is shown that the pipeline can benefit tremendously from this step. Experimental evaluation shows that our writer identification and writer retrieval pipeline is superior compared to the state-of-the-art pipelines, as our results on the publicly available ICDAR13 and CVL datasets set new standards by achieving 96.5% and 98.4% mAP, respectively.

1 Introduction

Along with biometrics identifiers such as DNA, fingerprints, and etc, handwriting is considered as special case of behavioral biometrics [30]. Handwriting analysis helps to extract attributes such as writer from a handwritten document. There are several factors that leads to handwriting variability such as using different pens, hurrying of writer, aging, and etc may result in varying styles of handwriting for each person. Thus, Handwriting analysis is complex and challenging task. In order to overcome these challenges and to provide an automatic handwriting analysis system, one needs to differentiate between *online* and *offline* data. Online text analysis systems capture the whole procedure of writing with special devices and the input consists of temporal data such as pen-tip positions. On the other hand, offline data is usually static and typically is in format of a image. Also, methods for handwriting analysis is categorized into to groups: *text-dependent* and *text-independent* methods. In text-dependent methods each handwriting must contain a fixed content, while in text-independent methods no assumptions made on the content of handwriting. In this work, it is intended to provide a offline text-independent handwriting analysis system concentrated on the problem of writer recognition, specifically writer identification and writer retrieval.

Writer retrieval is the task of ranking document images from a large corpus of data with similar handwriting to the *query* sample, See Figure 1a. Experts in relative fields then analyse these rankings and thus new documents from the same writer can be found. Historians and paleographers benefit the most from this scenario. When analysing historical documents, a vast amount of data should be dealt with, where examining them individually is not possible or a very time-consuming task. However, this scenario helps to find the writer of a historical document in a short list without having to go through all documents in the database. In contrast to writer retrieval, *writer identification* is the task of finding the writer of a query sample assuming a set of documents where each one's writer is *known* in advance, see Figure 1b. This scenario is often applicable in forensic sciences, e.g, finding the writer of a threatening letter.

The methods for both scenarios are similar. Both generate a feature vector describing the handwriting of each document with respect to its writer. These feature vectors are compared using a similarity measure such as cosine distance and then rankings are computed. For the retrieval scenario, these rankings are further analysed and a short list of documents written by the query's writer will

be returned. On the other hand, for the identification scenario, the writer of the sample with the shortest distance to the query sample is returned as output.

Our proposed pipeline uses a ResNet-20 convolutional neural network with the NetVLAD layer, inspired by Vectors of Locally Aggregated Descriptors (VLAD), to extract local descriptors and their corresponding embeddings describing small windows in a document image. Afterwards, generalised max-pooling (GMP) aggregation is employed to achieve a single global image descriptor for each image. Dimensionality reduced global image descriptors by means of PCA, are then compared and rankings are computed. In the final part, we make use of a re-ranking strategy based on query expansion and k -reciprocal nearest neighbours to improve retrieved rankings before evaluation.

The structure of this work is as follows: In Section 2 some deep-learning-based related work in the field of writer identification and retrieval, as well as re-rankings, are discussed. Afterwards, in Section 3 we investigate our proposed pipeline in great detail. Section 4 introduces datasets and finally, we evaluate and compare our proposed pipeline against state of the art on two different datasets (ICDAR13 and CVL) in Section 5.

2 Related Work

Nearly all common writer identification and retrieval datasets consist of writer disjoint train and test sets. Hence, an end-to-end training cannot be applied.

One of the first writer recognition methods using deep learning techniques was proposed by Fiel and Sablatnig [13]. They trained the "caffenet" CNN on line and word segmentations. Feature vectors extracted from the penultimate layer of the CNN are compared using the χ^2 -distance. At the time, their results showed superior performance on the IAM [26] and ICFHR'12 datasets while being inferior on the ICDAR13 [24] dataset. Christlein et al [4] used activation features of from a CNN as image local descriptors. Afterwards, global images descriptors are formed by means of GMM supervecor encoding. Their approach improved 0.21 % in terms of mAP on the ICDAR13 dataset. In another recent method by Christlein et al [7] LeNet and ResNet architectures are employed to extract local descriptors followed by VLAD encoding to compute global image descriptors for document images. They experimented with

arXiv:2012.06186v1 [cs.CV] 11 Dec 2020

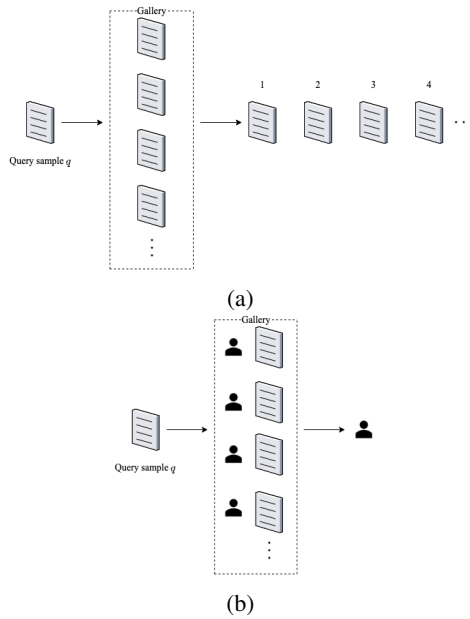


Fig. 1: (a) Overall schema of writer retrieval and (b) writer identification.

both exemplar support vector machines (ESVMs) and nearest neighbours to evaluate their pipeline. To the best of our knowledge, their approach has set new standards on the ICDAR13 and CVL [22] datasets.

In [21] Jordan et. al. experimented with reciprocal relationships in two ways. First, integrated them into the Jaccard distance and computed the final rankings based on a weighted sum of the original distance and the Jaccard distance. Second, encoded them into new feature vectors and hence expanded the positive set for ESVMs. As a result, their both techniques outperformed the baseline on the ICDAR17 dataset [14].

Tang and Wu [32] proposed a novel approach with convolutional neural network (CNN) and join Bayesian consisting of two stages: 1. feature extraction and 2. writer identification. They used CNNs to extract global features instead of small image patches. They used random word segmentations and generated 500 and 20 training samples per writer for training and testing, respectively. Finally, a Bayesian network used for computation of similarity between feature vectors. At the time, they achieved best results compared to state-of-the-art on ICDAR13 and CVL datasets. In another work by Xing and Qiao [34], two adjacent images patches used as inputs to their proposed network, named DeepWriter, consisting of two branches sharing the convolutional Layers. For the final evaluation part, two softmax layers belonging to each branch were averaged to predict the writer and achieved promising results on the IAM dataset. In spite of that, comparison of their work with other performances is impossible, since they splitted some lines of each writer into train, validation and test sets. In other words they used end-to-end training.

Consider that our proposed pipeline is mostly inspired by the works of Christlein et al [4, 7, 9] and Jordan et. al [21]. However, with our proposed pipeline consisting of the unified neural network architecture with the NetVLAD layer, and re-ranking strategy based query expansion and k -reciprocal nearest neighbors, we could improve upon the state-of-the-art on the ICDAR13 and CVL datasets.

3 Writer Identification Pipeline

Our proposed pipeline consists of two parts: 1. A unified neural network architecture with ResNet-20 [17, 18] and the NetVLAD layer [2], and 2. A re-ranking strategy to improve final results. The first part itself consists of three main steps (depicted in Figure 2): The ResNet-20 with the NetVLAD layer to extract local image

descriptors and their corresponding embeddings, An orderless aggregation function to pool obtained embeddings of each image into one global image descriptor, and the normalization and PCA [33] dimensionality reduction of resulted global image descriptors.

3.1 Convolutional Neural Network with NetVLAD Layer

State-of-the-art deep-learning-based methods in writer identification and retrieval use a CNN to extract local image descriptors which are subsequently encoded using an encoding method. An encoding consists of two steps: 1) An *embedding* step, where local feature vectors are projected into a possibly high-dimensional space, and 2) An *aggregation* step, in which embedded local feature vectors of each input image are pooled into one global image descriptor. Christlein et al [7] computed local feature vectors by means of ResNet-20 residual neural network and used the VLAD [20] encoding method for embedding and aggregation. Building on the success of Christlein et al [7] We propose a unified Neural network consisting of ResNet-20 followed by the trainable NetVLAD layer [2], inspired by the VLAD, at the head of the last convolutional layer of ResNet-20 to learn embedding of feature vectors in an end-to-end manner using a triplet loss [31].

3.1.1 ResNet-20 and NetVLAD: Details of the ResNet-20 convolutional neural network and the NetVLAD layer are described in following.

ResNet-20 Convolutional Neural Network. For network inputs, 32×32 image patches centered at the contour of handwriting were extracted. Same as Christlein et al [7] we follow the architectural design of He et al. [17] on CIFAR10 dataset [23]. $6n + 2$ layers are employed with n set to 3 leading to the ResNet-20 architecture. The first layer is 3×3 convolutions. Then an stack of $6n$ layers with 3×3 convolutions follows with every $2n$ layers forming an *stage*. At the beginning of each stage (except the first one), the feature map size is halved (downsampled) by a convolutional layer with the stride of 2, while the number of filters is doubled. Within each stage, the layers have the same number of filters. More precisely, feature maps and filters for stages are of sizes $\{32, 16, 8\}$ and $\{16, 32, 64\}$, respectively. Shortcut connections are connected to the pairs of 3×3 layers leading to a total $3n$ shortcuts. The network ends with the global average pooling layer with a size of 8 and an N -way fully connected layer. However, We discard the last fully-connected layer and pass the $1 \times 1 \times 64$ output feature vector global average pooling layer to the NetVLAD to further learn the VLAD embeddings of these feature vectors. (See Figure 3).

NetVLAD Layer. The idea behind the vectors of locally aggregated descriptors (VLAD) [20] is to compute the embeddings by means of residuals $x_i - c_k$ for each local image descriptor x_i . Finally, embedded local image descriptors of each image are accumulated by an orderless aggregation function. This characterizes the distribution of the vectors with respect to the cluster centers. The VLAD embedding can be regarded as simplified version of the Fisher Vectors [20]. More precisely, given N local image descriptors $\{x_i | x_i \in \mathbb{R}^D, i = 1, \dots, N\}$ and a dictionary of K cluster centers $\{c_j | c_j \in \mathbb{R}^D, j = 1, \dots, K\}$, the VLAD embedding function is computed as follows:

$$\phi_{\text{VLAD},k}(x_i) = \alpha_k(x_i)(x_i - c_k) \quad (1)$$

$$\alpha_k(x_i) = \begin{cases} 1, & \text{if } k = \operatorname{argmin}_{j=1, \dots, K} \|x_i - c_j\| \\ 0, & \text{else} \end{cases} \quad (2)$$

Then $\phi_{\text{VLAD}}(x_i) = (\phi_1(x_i), \dots, \phi_K(x_i))$ represents the full embedding for each local image descriptor x_i .

Arandjelovic et al [2] introduced a trainable generalized VLAD layer, named NetVLAD, which is pluggable into any CNN architecture. Local image descriptors clusters hard-assignments $a_k(x_i)$ in

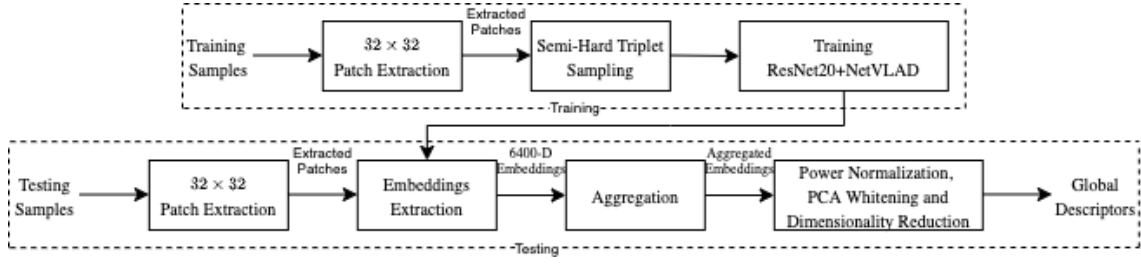


Fig. 2: Overview of proposed pipeline.

the original VLAD are the source of discontinuities and prevent differentiability in the learning procedure. The authors replaced them with soft-assignment to make it amenable to backpropagation:

$$\bar{\alpha}_k(x_i) = \frac{e^{-\alpha \|x_i - c_k\|^2}}{\sum_{j=1}^K e^{-\alpha \|x_i - c_j\|^2}} \quad (3)$$

where α is a parameter that control the decay of response with the magnitude of distance. Intuitively, Equation (3) assigns the weights of local image descriptors x_i proportional to their nearness to clusters c_j . Moreover, factorizing $e^{-\alpha \|x_i\|^2}$ results in:

$$\bar{\alpha}_k(x_i) = \frac{e^{w_k^T x_i + b_k}}{\sum_{j=1}^K e^{w_j^T x_i + b_j}} \quad (4)$$

where $w_k = 2\alpha c_k$ and $b_k = -\alpha \|c_k\|^2$. However, in [1] the authors propose decoupling dependencies of parameters c_k , w_k , and b_k as it will brings greater flexibility to the model. In this manner NetVLAD layer consists of three independent set of learnable parameters. We crop the ResNet-20 at the last convolutional layer and view it as a D -dimensional (here $D = 64$) local image descriptor. As depicted in Figure 3 the NetVLAD layer can be decomposed into CNN layers connected in an acyclic graph. Equation (4) represents the soft-max activation function. So the soft-assignments of local image descriptor x_i to clusters c_k can be viewed as applying a 1×1 convolution layer with K filters representing w_k and biases as b_k followed by the soft-max activation function to obtain final soft-assignments $\bar{\alpha}_k(x_i)$. The final output is $K \times D \times 1$ -dimensional representing the full embedding for local image descriptor x_i .

The authors in [1] regard the output of the last convolutional layer with $H \times W \times D$ map as a set of D -dimensional descriptors at $H \times W$ spatial locations in input image which are further embedded and pooled by the NetVLAD layer. However, by using ResNet-20 with image patches of size 32×32 as feature extractor, output of the last convolutional layer becomes $1 \times 1 \times 64$ map which we consider as 64-dimensional local image descriptor extracted from the input image patch. Passing this descriptor (with $H = 1$ and $W = 1$) enables NetVLAD layer to learn the respective local image descriptor embedding. So in this manner, the NetVLAD layer functions as generalized VLAD embedding. ℓ_2 -normalization is employed prior to learning from semi-hard triplets.

Learning from Semi-Hard Triplets. We wish to learn VLAD embedding representation $\phi_{\text{VLAD}}(x)$ constrained to lie on $K \times D$ -dimensional hypersphere, i.e. $\|\phi_{\text{VLAD}}(x)\| = 1$, such that two embeddings belonging to the image(s) of the same writer be close together in the embedding space while embeddings of images with different writers lie far away from each other. However, we don't want to push the train embeddings of images each writer to collapse into very small clusters. The only requirement is that given two positive embeddings of the same writer and one negative embedding, the negative should be farther away than the positive by some margin m . This requirement can be translated into a loss between triplets. The loss will be defined over triplets of embeddings: an anchor ϕ_a , a positive of the same writer as the anchor ϕ_p , and a negative of a

different writer ϕ_n . For some distance on the embedding space d , the loss of a triplets (ϕ_a, ϕ_p, ϕ_n) is:

$$\mathcal{L} = \max(d(\phi_a, \phi_p) - d(\phi_a, \phi_n) + \text{margin}, 0) \quad (5)$$

The original NetVLAD paper utilizes the weakly supervised triplet ranking loss [2]. However, Since here the NetVLAD layer is applied to learn patch-wise embeddings, Another strategy is employed. Based on the definition of loss we tend to train on semi-hard triplets [31]: triplets where the negative is not closer to the anchor than the positive, but which still produce positive loss: $d(\phi_a, \phi_p) < d(\phi_a, \phi_n) < d(\phi_a, \phi_p) + \text{margin}$.

We train parameters of proposed pipeline on large set of semi-hard triplets image patches triplets extracted from the respective dataset. Details and parameters of training are given in Section 4.

3.1.2 Aggregation: Aggregation step is required to obtain a single vector representing each image from its embedded local descriptors. Default aggregation method is *sum-pooling*. Assuming the set of N local descriptors $\mathcal{X} = \{x_i | i = 1, \dots, N\}$ for an image, sum-pooling constructs global descriptor ξ as follows:

$$\xi = \psi(\phi(\mathcal{X})) = \sum_{x \in \mathcal{X}} \phi(x). \quad (6)$$

"Since we sum over all descriptors, the aggregated descriptors can suffer from interference of unrelated descriptors that influence the similarity, even if they have low individual similarity" [8] as the similarity $\mathcal{K}(\mathcal{X}, \mathcal{Y})$ between two images represented by sets \mathcal{X} and \mathcal{Y} is computed as follows:

$$\mathcal{K}(\mathcal{X}, \mathcal{Y}) = \sum_{x \in \mathcal{X}} \sum_{y \in \mathcal{Y}} \phi(x) \cdot \phi(y). \quad (7)$$

Hence, more frequently occurring descriptors will be more influential in the final representation and affect the final similarity between global descriptors. This phenomenon is called *visual burstiness* [19]. Recently, a novel approach named *generalized max-pooling* [27] was proposed to overcome this problem and has successfully applied in field of writer identification and retrieval in works of Christlein et al [7]. We employed this method in our pipeline as it has shown superior performance to the other two methods [28]. Generalized max-pooling balances contribution of every embedding $\phi(x) \in \mathbb{R}^{K \times D}$ where $x \in \mathbb{R}^D$ is local image descriptor, by solving a ridge regression problem. Therefore,

$$\phi(x)^T \xi_{gmp}(\mathcal{X}) = C, \quad \forall x \in \mathcal{X}, \quad (8)$$

where \mathcal{X} is the set of all local descriptors of an image, ξ_{gmp} denotes aggregated global image descriptor and C is a constant that can be set arbitrarily since it has no influence as the global image descriptors sine they are subsequently normalized in the post-processing

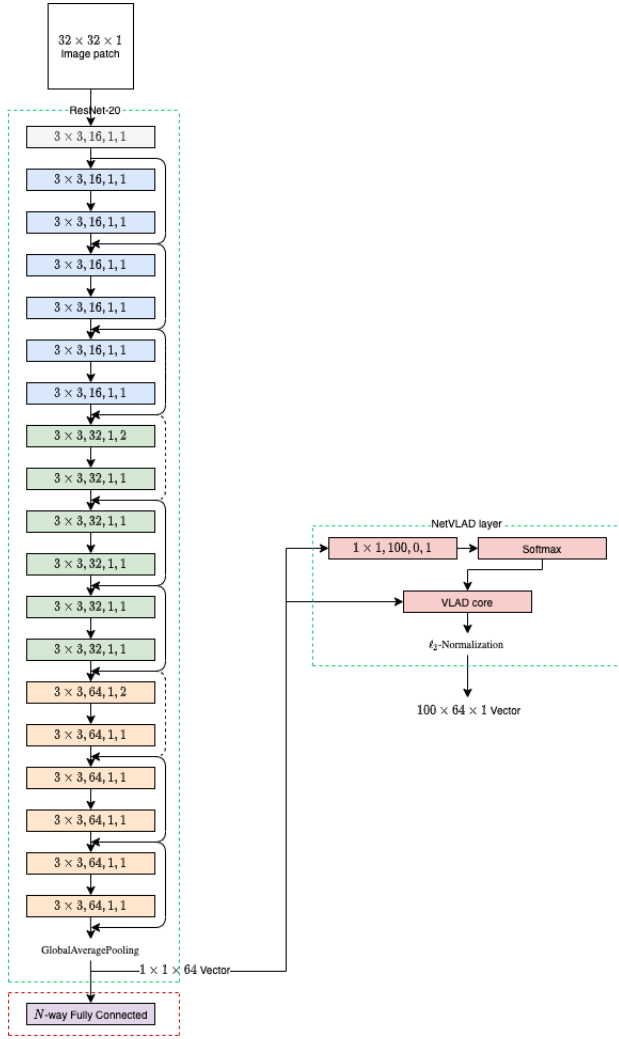


Fig. 3: CNN architecture composed of the ResNet-20 followed by the NetVLAD layer. Numbers in each rectangle denote *kernel size, number of output filters, padding, and size of stride*, respectively. The N -way fully connected is dropped and instead the $1 \times 1 \times 64$ output vector is passed to the NetVLAD layer.

step. Equation (8) can be re-formulated for the all N local image descriptors of each image as below:

$$\Phi^T \xi_{gmp} = \mathbf{1}_N, \quad (9)$$

where Φ and $\mathbf{1}_N$ denote the $(K \times D) \times N$ matrix of all local image descriptors embeddings and vector of N constants set to 1, respectively. Equation (9) can be turned into a least-squares ridge regression problem [7, 9]:

$$\xi_{gmp} = \underset{\xi}{\operatorname{argmin}} \|\Phi^T \xi - \mathbf{1}_N\|_2^2 + \lambda \|\xi\|_2^2 \quad (10)$$

with λ being a regularization parameter. In the remainder of this work, ψ denotes the aggregated global image descriptor.

3.1.3 Normalization and Dimensionality Reduction: While working with global image descriptors obtained in the previous step, two challenges arise: 1. visual burstiness might corrupt visual similarity measure between global image descriptors, i.e. the cosine distance used to rank images and 2. These global descriptors lie in a very high-dimensional space and pipeline might benefit from projecting them to a lower-dimensional space. We address these challenges with an additional normalization and dimensionality reduction step.

Power Normalization. A normalization method to counter visual burstiness is named *power normalization* [29] that proposes to apply function f component-wise to global image descriptor ψ ,

$$f(\psi) = \operatorname{sign}(\psi_i) |\psi_i|^p, \quad \forall i, 1 \leq i \leq n \quad (11)$$

where p is a normalization parameter and is generally is set to 0.5. Power normalization is followed by ℓ_2 -normalization.

Principal Component Analysis. Due to the nature of VLAD encoding, global image descriptors lie in a very high-dimensional space. Principal component analysis (PCA) [33] is used to dimensionality reduce the encoding representations. However, this introduces a new parameter, *dimension*, to the pipeline denoting the number of components to keep. After performing the PCA, ℓ_2 -normalization along each sample is necessary.

3.2 Re-ranking

Writer identification and retrieval systems are evaluated using leave-one-image-out cross validation. Each image is once used as *query* q and the pipeline returns a ranked list $L(q)$ of all other images in test set (a.k.a *gallery*). These ranked lists are obtained by computing the pairwise distance between query q and each $p \in L(q)$ using a similarity measure, i.e. *cosine distance*. Given two vectors p a q , the cosine distance is defined as:

$$d_{\cos}(p, q) = 1 - \frac{pq}{\|p\| \|q\|}. \quad (12)$$

Our goal is to re-rank each $L(q)$ based on knowledge lied in it, so that more *relevant* samples rank top in the list and thus, boost the performance of writer identification and retrieval.

3.2.1 Nearest Neighbors: k -nearest neighbors $k\text{NN}(q)$ (top- k ranked samples of ranked list) of query q is defined as:

$$k\text{NN}(q) = \{p_1, p_2, \dots, p_k\}, \quad |k\text{NN}(q)| = k, \quad (13)$$

Where $|\cdot|$ denotes the cardinality of the set. The k -reciprocal nearest neighbors $k\text{rNN}(q, k)$ is defined as:

$$k\text{rNN}(q) = \{p_i | p_i \in k\text{NN}(q) \wedge q \in k\text{NN}(p_i)\}. \quad (14)$$

In other words, two samples q and p are considered as k -reciprocal nearest neighbors, when both appear within the top- k ranked samples of each other. According to the previous descriptions, k -reciprocal nearest neighbors are more related to query q than k -nearest neighbors.

3.2.2 Query Expansion and k -Reciprocal Nearest Neighbors:

A common approach in order to boost performance of information retrieval systems is automatic query expansion (QE) [21]. With an initial ranked lists $L(q)$ computed, query expansion reformulates each query sample q and obtains the improved ranked list by re-querying using the newly formed query instead of q .

Chum et al [10] proposed the following query expansion approach. For query q , a new query sample can be formed by taking average over top- n spatially verified samples \mathcal{F} from ranked list $L(q)$,

$$q_{\text{avg}} = \frac{1}{|\mathcal{F}| + 1} \left(q + \sum_{f \in \mathcal{F}} f \right) \quad (15)$$

where f_i and n denote the i th sample in \mathcal{F} and total number of samples in $|\mathcal{F}|$, respectively.

In our problem, the features do not encode any global spatial information and thus, we have no spatial verification at hand. Averaging over top- k samples in $L(q)$ is not much reliable since the top- k samples might contain false matches. We propose to use a more constrained strategy by taking an average over query q and its k -rNNs in the initial ranked list to minimizing the risk of including

All the world's a stage, and all the men and women
merely players: they have their exits and their entrances;
and one man in his time plays many parts, his acts
being seven ages.

Fig. 4: Example document sample from the ICDAR13 dataset (ID:032_1)

When we look to the individuals of same variety or sub-variety
of our older cultivated plants and animals, one of the first
points to which strikes us, is, that they generally differ much
more from each other, than do the individuals of any one
species or variety in a state of nature.

Fig. 5: Example document sample from the CVL dataset (ID:0073-4).

false matches. Hence, the newly formed query q_{new} is computed as follows:

$$q_{\text{new}} = \frac{1}{|\text{krNN}(q)| + 1} \left(q + \sum_{r \in \text{krNN}(q)} r \right). \quad (16)$$

This however introduces a new hyper-parameter k to the pipeline. In following, our proposed pipeline (with re-ranking) is denoted as "Proposed(+krNN-QE $_k$)".

4 Evaluation

4.1 Datasets

Our primary dataset is the ICDAR13. However, we compare our results against state of the art on the CVL dataset as well.

ICDAR13 The ICDAR13 dataset is introduced for the ICDAR 2013 competition on writer identification [24]. It consists of four samples per writer, two of which are written in English while the two others are written in Greek. The dataset is composed of disjoint training (a.k.a experimental) and test (a.k.a benchmarking) sets. The training set consists of 100 writers and the testing set comprises of 250 writers. Example documents from ICDAR 2013 dataset can be seen in Figure 4.

CVL The CVL dataset [22] (version 1.1) consists of 27 writers contributing to seven texts (one in German and six in English) in the officially provided train set. The test set comprises of 283 writers where each has copied five texts (one in German and four in English). Two of the document samples from this dataset is shown in Figure 5.

4.2 Metrics

Results are reported in terms of the Hard Top- N and mAP which are defined in following.

Hard Top- N , The strictest evaluation metric is hard top- N . A returned list $L(q)$ for query sample q is considered as *acceptable* [3] if all of the top- N ranked samples in $L(q)$ belong to the same class as sample q 's class i.e., written by same writer. The ratio of the number of acceptable returned lists and the number of query samples is reported as Hard Top- N accuracy.

Mean Average Precision. Another commonly used measure to evaluate an information retrieval task is the mean average precision (mAP) which considers the ranking of correct samples. It is calculated as the mean over all examined query samples q of set \mathcal{Q} :

$$\text{mAP} = \frac{\sum_{q \in \mathcal{Q}} \text{AveP}(q)}{|\mathcal{Q}|}, \quad (17)$$

where $\text{AveP}(q)$ is the average precision for a given query q defined as below:

$$\text{AveP}(q) = \frac{\sum_{k=1}^n (P(k) \times \text{rel}(k))}{\text{number of relevant documents}}, \quad (18)$$

where n is the total number of retrieved samples, $\text{rel}(k)$ is a binary function returning 1 if sample at rank k of $L(q)$ is relevant and 0 otherwise, and $P(k)$ is the precision at rank k (fraction of relevant items up to first k retrieved samples in $L(q)$).

4.3 Experiments and Results

Most datasets in the field of writer identification and retrieval come with disjoint train and test sets. Therefore, Our pipeline is composed of two phases: (1) training phase and (2) testing phase, each described below. Note that since the official train set of the CVL dataset is rather small (189 samples), we evaluate on the CVL test set using the ICDAR13 train set.

Training phase. To train and validate the neural network, 32×32 patches centered on the contour of handwritten images in the ICDAR13 train set are extracted. We sample around 500000/25000 image patches for train/validation which are subsequently passed forward to the network. ResNet weights are initialized by *He-initialization* [16] and *Xavier-intilization* [15] used to initialize Conv layer of the NetVLAD. As the ICDAR13 test set consists of 100 writers, the number of cluster centers has been set to 100 in the NetVLAD layer. The proposed neural network is optimized using Adamax with respect to triplet semi-hard loss with margin $m = 0.1$, decay rates $\beta_1 = 0.9$ and $\beta_2 = 0.99$ for 1st moment estimate and exponentially weighted infinity norm, respectively. Training is stopped after 5 epochs since the loss value stagnated at this point. The Visualization of learning curves can be seen in Figure 6.

Testing Phase. Once the proposed network is trained, we pass image patches of respective test set to obtain embedded feature vectors which eventually are pooled to construct global image descriptors of each image. For generalized max-pooling, following the works of Christlein et. al. [7] we set $\lambda = 1000$. PCA used for whitening and projecting global descriptors to a user-defined number of *deminesions* (Figure 8 shows the mAP for the different number of *deminesions* on ICDAR13 test set) and they are subsequently ℓ_2 -normalized. To have a clear view of how the proposed pipeline can benefit from re-ranking, Table 1 provides a comparison between the proposed pipeline with initial rankings (denoted as "Proposed") and re-ranking with different values for k (denoted as "Proposed+krNN-QE $_k$ "). Observations reveal that *dimension* = 128 and $k = 2$ give the best results on the ICDAR13 test set.

4.3.1 Visualisation of Embeddings: There are 400 extracted 128- D dimensional global image descriptors from the ICDAR13 train set after performing normalization and dimensionality reduction. We further reduced their dimensionality using t-SNE [25] projection for visualisation purposes. The t-SNE plot of the embeddings space is shown in Figure 8. The plot shows that the embeddings learned by the proposed pipeline has very good discriminative properties as every 4 global images descriptors of each writer approximately lie near each other. In other words, nearest neighbours of each global images descriptor stem from the same writer. On the other hand, Figure 9 depicts 1000 global image descriptors of dimension 128 of ICDAR13 test set before and after re-ranking part. As the

Table 1 Comparison of evaluation with initial rankings against re-ranking with different values of k on ICDAR13 test set.

	Top-1	Hard-2	Hard-3	mAP
Proposed	98.60	84.10	65.60	93.01
Proposed+krNN-QE _{$k=1$}	98.70	90.30	86.70	96.48
Proposed+krNN-QE _{$k=2$}	97.90	90.50	86.80	96.58
Proposed+krNN-QE _{$k=3$}	96.40	91.00	83.50	96.36

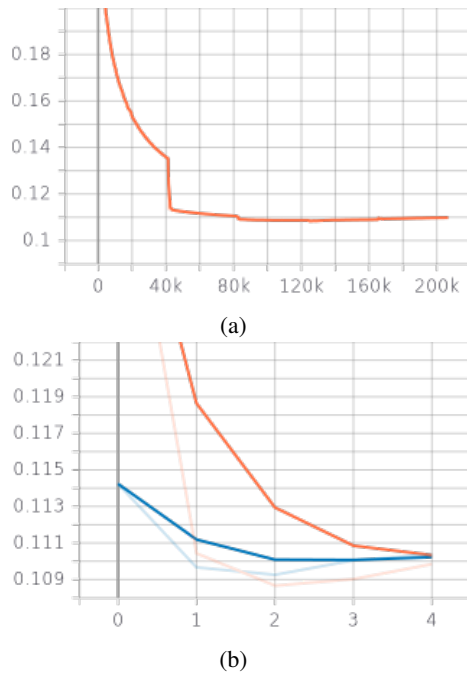


Fig. 6: (a) Training learning curve in terms of batch number, and (b) based on epoch number. Orange and Blues denotes train and validation curves, respectively.

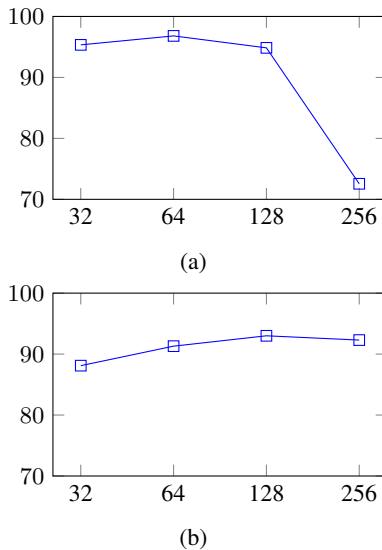


Fig. 7: Comparison of effect of number of components in PCA in terms of mAP on (a) ICDAR13 train set and (b) ICDAR13 test set.

Figure illustrates, discriminativity of clusters are increased and the clusters belonging to each writer are more distinguishable from each other.

4.3.2 Comparison with State of the Art: Finally, we compare our results (Proposed+krNN-QE _{$k=2$}) with state of the art on the

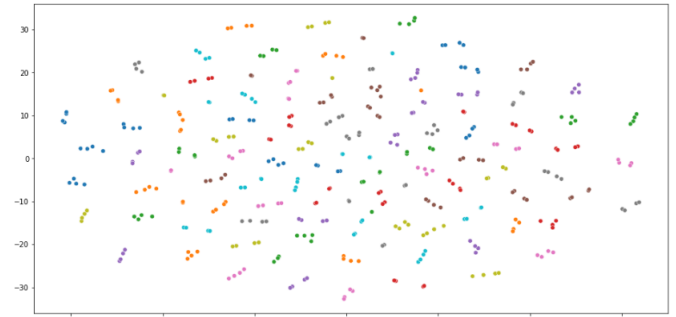


Fig. 8: t-SNE plot of the ICDAR13 train set global descriptors. There are 100 colours each representing document images of unique writer.

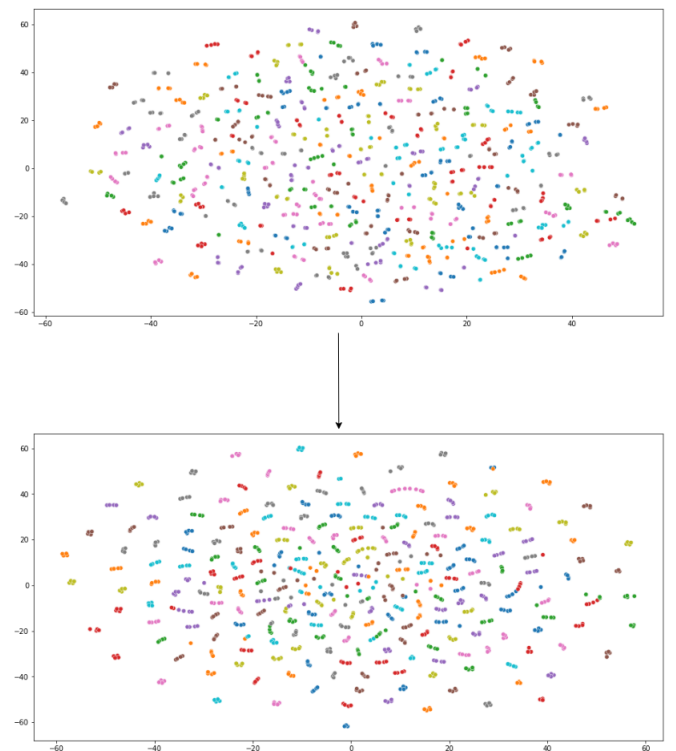


Fig. 9: t-SNE plot of ICDAR13 test set global descriptors before (above Figure) and after re-ranking (below Figure) with $k = 2$.

ICDAR13 and CVL contemporary datasets. We give results in terms of mAP, Top-1, Hard-2, and Hard-3 metrics. Top-1 gives the probability that the first retrieved item belongs to the same writer, While Hard-2 and Hard-3 are the probabilities that all top two and three ranked results stem from the same writer, respectively. ResNet-20 with the NetVLAD is used to extract local descriptors followed by generalized max-pooling in order to form a global descriptor for each image. Afterward, ℓ_2 -normalization as well as SSR are applied on these descriptors which are further dimensionality reduced to 128-D by means of PCA.

Table 2 Evaluation of ICDAR13 dataset. Numbers taken from [9].

Method	Top-1	Hard-2	Hard-3	mAP
Fiel & Sablatnig [11]	90.9	44.8	24.5	-
Fiel & Sablatnig [13]	88.5	63.2	36.5	-
Fiel [12]	96.8	42.3	23.1	-
Tang & Wu [32]	99.0	84.4	68.1	-
Christlein et al [3]	97.1	42.8	23.8	67.1
Christlein et al [6]	99.7	84.8	63.5	89.4
Christlein et al [9]	99.0	85.3	68.6	90.2
Christlein et al [9] + ESVM	99.6	89.8	77.0	93.2
Proposed+krNN-QE _{k=2}	97.9	90.5	86.8	96.5

Table 3 Evaluation of CVL dataset using ICDAR13 train set. Numbers taken from [9].

Method	Top-1	Hard-2	Hard-3	mAP
Christlein et al [3]	99.2	98.1	95.8	97.1
Christlein et al [4]	99.4	98.8	97.3	97.8
Christlein et al [5]	99.4	98.9	97.4	97.9
Christlein et al [6]	99.2	98.4	97.1	98.0
Christlein et al [9]	99.2	98.4	95.9	97.1
Christlein et al [9] + ESVM	99.3	98.7	97.0	97.8
Proposed+krNN-QE _{k=2}	98.8	98.4	97.5	98.4

ICDAR 2013. Comparison of our results on ICDAR13 dataset are provided in table 2. Our method with the proposed re-ranking strategy achieves the overall best result (in terms of mAP) with a 3.3% difference against the previous best [9]. Also, the Hard-3 metric is improved 10.2% which is an indicator of the huge benefit that re-ranking brings to the pipeline. This can also be seen on Hard-2 that shows slightly better results. However, inferior performance obtained in terms of Top-1.

CVL Dataset. For the evaluation of the CVL dataset, we used the official test split, i.e. containing the subset of writers where each contributed exactly five forms (CVL-283). However, since the training set is rather small (189 samples), so we have used the ICDAR13 training set. The obtained results compared with state of the art are given in table 3. Our proposed approach with re-ranking sets new standards by showing superior performance in terms of Hard-3 and mAP on the CVL dataset.

5 Conclusion

In this work, we have presented a 1) novel pipeline consisting of a convolutional neural network followed by the NetVLAD layer to extract local descriptors and their corresponding VLAD embeddings in an end-to-end manner and 2) re-ranking strategy based on query expansion and k -reciprocal nearest neighbors to improve initial rankings.

Our results demonstrate improvements and set new standards on both ICDAR13 and CVL datasets. However, there is still room for improvement in various directions. The preprocessing step could be investigated in more detail. Also, deep learning-based approaches other than NetVLAD such as DeepTen [35] may worth investigating. On the other hand, we have used the NetVLAD layer to extract embeddings but employing it to directly learn global image descriptors could also be beneficial. Finally, historical data are getting more and more attention in recent years, so for future works, the application of the proposed pipeline on historical data must be researched.

6 Acknowledgment

The second author thanks Professor Patrick Wambacq from KU Leuven for his valuable scientific discussions that have contributed to improving the quality of this work.

7 Conflict of Interest

The authors have no conflict of interest to declare.

8 References

- Arandjelovic, R. and Zisserman, A., 2013. All about VLAD. In Proceedings of the IEEE conference on Computer Vision and Pattern Recognition (pp. 1578-1585).
- Arandjelovic, R., Gronat, P., Torii, A., Pajdla, T. and Sivic, J., 2016. NetVLAD: CNN architecture for weakly supervised place recognition. In Proceedings of the IEEE conference on computer vision and pattern recognition (pp. 5297-5307).
- Christlein, V., Bernecker, D., Höning, F. and Angelopoulou, E., 2014, March. Writer identification and verification using GMM supervectors. In IEEE Winter Conference on Applications of Computer Vision (pp. 998-1005). IEEE.
- Christlein, V., Bernecker, D., Maier, A. and Angelopoulou, E., 2015, October. Offline writer identification using convolutional neural network activation features. In German Conference on Pattern Recognition (pp. 540-552). Springer, Cham.
- Christlein, V., Bernecker, D. and Angelopoulou, E., 2015, August. Writer identification using VLAD encoded contour-Zernike moments. In 2015 13th International Conference on Document Analysis and Recognition (ICDAR) (pp. 906-910). IEEE.
- Christlein, V., Bernecker, D., Höning, F., Maier, A. and Angelopoulou, E., 2017. Writer identification using GMM supervectors and exemplar-SVMs. Pattern Recognition, 63, pp.258-267.
- Christlein, V. and Maier, A., 2018, April. Encoding CNN activations for writer recognition. In 2018 13th IAPR International Workshop on Document Analysis Systems (DAS) (pp. 169-174). IEEE.
- Christlein, V., Spranger, L., Seuret, M., Nicolaou, A., Král, P. and Maier, A., 2019, September. Deep Generalized Max Pooling. In 2019 International Conference on Document Analysis and Recognition (ICDAR) (pp. 1090-1096). IEEE.
- Christlein, V.: Handwriting analysis with focus on writer identification and writer retrieval. PhD thesis, Friedrich-Alexander-Universität Erlangen-Nürnberg, 2019.
- Friedrich-Alexander-Universität Erlangen-Nürnberg, O., Philbin, J., Sivic, J., Isard, M. and Zisserman, A., 2007, October. Total recall: Automatic query expansion with a generative feature model for object retrieval. In 2007 IEEE 11th International Conference on Computer Vision (pp. 1-8). IEEE.
- Fiel, S. and Sablatnig, R., 2013, August. Writer identification and writer retrieval using the fisher vector on visual vocabularies. In 2013 12th International Conference on Document Analysis and Recognition (pp. 545-549). IEEE.
- Fiel, S.: Novel methods for writer identification and retrieval. PhD thesis, Technische Universität Wien, 2015.
- Fiel, S. and Sablatnig, R., 2015, September. Writer identification and retrieval using a convolutional neural network. In International Conference on Computer Analysis of Images and Patterns (pp. 26-37). Springer, Cham.

- 14 Fiel, S., Kleber, F., Diem, M., Christlein, V., Louloudis, G., Nikos, S. and Gatos, B., 2017, November. Icdar2017 competition on historical document writer identification (historical-wi). In 2017 14th IAPR International Conference on Document Analysis and Recognition (ICDAR) (Vol. 1, pp. 1377-1382). IEEE.
- 15 Glorot, X. and Bengio, Y., 2010, March. Understanding the difficulty of training deep feedforward neural networks. In Proceedings of the thirteenth international conference on artificial intelligence and statistics (pp. 249-256).
- 16 He, K., Zhang, X., Ren, S. and Sun, J., 2015. Delving deep into rectifiers: Surpassing human-level performance on imagenet classification. In Proceedings of the IEEE international conference on computer vision (pp. 1026-1034).
- 17 He, K., Zhang, X., Ren, S. and Sun, J., 2016. Deep residual learning for image recognition. In Proceedings of the IEEE conference on computer vision and pattern recognition (pp. 770-778).
- 18 He, K., Zhang, X., Ren, S. and Sun, J., 2016, October. Identity mappings in deep residual networks. In European conference on computer vision (pp. 630-645). Springer, Cham.
- 19 Jégou, H., Douze, M. and Schmid, C., 2009, June. On the burstiness of visual elements. In 2009 IEEE Conference on Computer Vision and Pattern Recognition (pp. 1169-1176). IEEE.
- 20 Jégou, H., Perronnin, F., Douze, M., Sánchez, J., Perez, P. and Schmid, C., 2011. Aggregating local image descriptors into compact codes. IEEE transactions on pattern analysis and machine intelligence, 34(9), pp.1704-1716.
- 21 Jordan, S., Seuret, M., Král, P., Lenc, L., Martínek, J., Wiermann, B., Schwinger, T., Maier, A. and Christlein, V., 2020, July. Re-Ranking for Writer Identification and Writer Retrieval. In International Workshop on Document Analysis Systems (pp. 572-586). Springer, Cham.
- 22 Kleber, F., Fiel, S., Diem, M. and Sablatnig, R., 2013, August. Cvl-database: An off-line database for writer retrieval, writer identification and word spotting. In 2013 12th international conference on document analysis and recognition (pp. 560-564). IEEE.
- 23 Krizhevsky, A. and Hinton, G., 2009. Learning multiple layers of features from tiny images.
- 24 Louloudis, G., Gatos, B., Stamatopoulos, N. and Papandreou, A., 2013, August. Icdar 2013 competition on writer identification. In 2013 12th International Conference on Document Analysis and Recognition (pp. 1397-1401). IEEE.
- 25 Maaten, L.V.D. and Hinton, G., 2008. Visualizing data using t-SNE. Journal of machine learning research, 9(Nov), pp.2579-2605.
- 26 Marti, U.V. and Bunke, H., 2002. The IAM-database: an English sentence database for offline handwriting recognition. International Journal on Document Analysis and Recognition, 5(1), pp.39-46.
- 27 Murray, N. and Perronnin, F., 2014. Generalized max pooling. In Proceedings of the IEEE conference on computer vision and pattern recognition (pp. 2473-2480).
- 28 Murray, N., Jégou, H., Perronnin, F. and Zisserman, A., 2016. Interferences in match kernels. IEEE transactions on pattern analysis and machine intelligence, 39(9), pp.1797-1810.
- 29 Perronnin, F., Sánchez, J. and Mensink, T., 2010, September. Improving the fisher kernel for large-scale image classification. In European conference on computer vision (pp. 143-156). Springer, Berlin, Heidelberg.
- 30 Schomaker, L., 2008. Writer identification and verification. In Advances in Biometrics (pp. 247-264). Springer, London.
- 31 Schroff, F., Kalenichenko, D. and Philbin, J., 2015. Facenet: A unified embedding for face recognition and clustering. In Proceedings of the IEEE conference on computer vision and pattern recognition (pp. 815-823).
- 32 Tang, Y. and Wu, X., 2016, October. Text-independent writer identification via CNN features and joint Bayesian. In 2016 15th International Conference on Frontiers in Handwriting Recognition (ICFHR) (pp. 566-571). IEEE.
- 33 Wold, S., Esbensen, K. and Geladi, P., 1987. Principal component analysis. Chemometrics and intelligent laboratory systems, 2(1-3), pp.37-52.
- 34 King, L. and Qiao, Y., 2016, October. Deepwriter: A multi-stream deep CNN for text-independent writer identification. In 2016 15th International Conference on Frontiers in Handwriting Recognition (ICFHR) (pp. 584-589). IEEE.
- 35 Zhang, H., Xue, J. and Dana, K., 2017. Deep ten: Texture encoding network. In Proceedings of the IEEE conference on computer vision and pattern recognition (pp. 708-717).